



Study of Wave Propagation at Interface of Micropolar Elastic Solid and Micropolar Fluid Saturated Porous Solid

N. Kumari¹, R.K. Poonia², P. Kumar¹ and V. Kaliraman¹

¹Department of Mathematics, Chaudhary Devi Lal University, Sirsa, (Haryana), India.
²Department of Mathematics, Chandigarh University, Gharuan, Mohali, (Punjab), India.

(Corresponding author: P. Kumar)

(Received 02 May 2019, Revised 10 July 2019, Accepted 08 August 2019)

(Published by Research Trend, Website: www.researchtrend.net)

ABSTRACT: In this research article, more characteristic of amplitude ratios of assortment of reflected and refracted wave at the interface between micropolar elastic solid and micro polar fluid saturated porous solid have been investigated. So, the wave propagates in the medium micro polar elastic solid and micro polar fluid saturated porous solid and separated by an interface $z = 0$ is studied. Longitudinal wave and coupled wave impinges obliquely on plane boundary and calculate the amplitude ratios of different waves for this specific model and results obtained are revealed figures wise with respect to incidence angle.

Keywords: Micro polar elastic solid, porous solid, reflected waves, refracted waves, amplitude ratio.

I. INTRODUCTION

The structure of the Earth is complex and it involves materials of different kind. Liquid -saturated porous solids are often present on and below the surface of the Earth. Dynamic analysis of liquid-saturated porous media is a subject with applications in numerous branches of science and engineering, including geophysics, seismology, civil and mechanical engineering. Eringen and Suhubi [1] discovered "The theory of micropolar elasticity". In classical elasticity, the motion of atom is describe by displacement vector with three degree of freedom, while in micropolar elasticity, six degree of freedom of a particle which is in motion described by both of displacement vector and microrotation vector. Eringen [2] manufactured. "The linear theory of micropolar viscoelasticity". Lot of researchers analysed about the waves problems. Many of them are Parfitt and Eringen [3], Nowacki [4], Tomar and Kumar [5], Kumari [6], Barak *et al.*, [7], Merkel and Luding[8] and Kumari *et al.*, [9], Kumar *et al.*, [10-14], Madan *et al.*, [15-17] and Kaliraman and Poonia [18] etc. The theory of propagation of waves through the liquid saturated porous medium was discovered by Biot [19]. Consequently, Biot [20] discussed the general solution of equations for elasticity and consolidation for the porous materials.

The intention of the present paper is cogitation of propagation of waves at solid media. The amplitude ratios of are computed using appropriate boundary conditions and revealed figures wise with respect to incidence angle.

II. GOVERNING EQAUTIONS OF THE CONSIDERED PROBLEM

Medium M_1 (Micropolar elastic solid)

Eringen [21], derived the equations of the medium micropolar elastic solid.

$$(c_1^2 + c_3^2)\nabla^2\phi = \frac{\partial^2\phi}{\partial t^2} \quad (1)$$

$$(c_2^2 + c_3^2)\nabla^2U + c_3^2\nabla \times \Phi = \frac{\partial^2U}{\partial t^2} \quad (2)$$

$$(c_4^2\nabla^2 - 2\omega_0^2)\Phi + \omega_0^2\nabla \times U = \frac{\partial^2\Phi}{\partial t^2} \quad (3)$$

where

$$\begin{aligned} c_1^2 &= \frac{\lambda + 2\mu}{\rho} & c_2^2 &= \frac{\mu}{\rho} \\ c_3^2 &= \frac{\kappa}{\rho} & c_4^2 &= \frac{\gamma}{\rho_j} \\ \omega_0^2 &= \frac{\kappa}{\rho_j} \end{aligned} \quad (4)$$

Parfitt and Eringen [3], derived the equation (1) to longitudinal wave with velocity $V_1^2 = (c_1^2 + c_3^2)$ and Eqns. (2, 3) are coupled equations in vector potentials U and Φ and these correspond to coupled transverse and micro-rotation waves. If $\frac{\omega^2}{\omega_0^2} > 20, \exists$ two sets of coupled-wave propagating with velocities $1/\lambda_1$ and $1/\lambda_2$.

where

$$\lambda_2^2 = \frac{1}{2} [B + \sqrt{B^2 - 4C}] \quad \lambda_1^2 = \frac{1}{2} [B + \sqrt{B^2 - 4C}] \quad (5)$$

and

$$\begin{aligned} B &= \frac{q(p-2)}{\omega^2} + \frac{1}{(c_2^2 + c_3^2)} + \frac{1}{c_4^2} \\ C &= \left(\frac{1}{c_4^2} - \frac{2q}{\omega^2} \right) \frac{1}{(c_2^2 + c_3^2)} \\ p &= \frac{\kappa}{\mu + \kappa} & q &= \frac{\kappa}{\gamma} \end{aligned} \quad (6)$$

Considering the components of displacement and micro-rotation as

$$U = (u, 0, w) \quad \Phi = (0, \Phi_2, 0) \quad (7)$$

where

$$u = \frac{\partial\phi}{\partial x} - \frac{\partial\psi}{\partial z} \quad w = \frac{\partial\phi}{\partial z} + \frac{\partial\psi}{\partial x} \quad (8)$$

Stresses for medium M_1 are taken from Kumari [6].

Medium M₂ (Micropolar Fluid Saturated Porous Solid)

The fundamental equations for micro polar fluid saturated porous solid in the presence of extra vugance are given by Erigena [21] as

$$(\bar{\lambda} + 2\bar{\mu} + \bar{\kappa})\nabla(\nabla \cdot \bar{\mathbf{u}}) - (\bar{\mu} + \bar{\kappa})\nabla \times (\nabla \times \bar{\mathbf{u}}) + \bar{\kappa}(\nabla \times \bar{\Phi}) + \bar{Q}\nabla(\nabla \cdot \bar{\mathbf{u}}) = \frac{\partial^2}{\partial t^2}(\bar{\rho}_{11}\bar{\mathbf{u}} + \bar{\rho}_{12}\bar{\mathbf{U}}) + \bar{b}\frac{\partial}{\partial t}(\bar{\mathbf{u}} - \bar{\mathbf{U}}) \quad (9)$$

$$\nabla(\bar{Q}\bar{\mathbf{e}} + \bar{R}\bar{\mathbf{e}}) = \frac{\partial^2}{\partial t^2}(\bar{\rho}_{11}\bar{\mathbf{u}} + \bar{\rho}_{12}\bar{\mathbf{U}}) - \bar{b}\frac{\partial}{\partial t}(\bar{\mathbf{u}} - \bar{\mathbf{U}}) \quad (10)$$

$$(\bar{\alpha} + \bar{\beta} + \bar{\gamma})\nabla(\nabla \cdot \bar{\Phi}) - \bar{\gamma}\nabla \times (\nabla \times \bar{\Phi}) + \bar{\kappa}(\nabla \times \bar{\mathbf{u}}) - 2\bar{\kappa}\bar{\Phi} = \bar{\rho}\frac{\partial^2 \bar{\Phi}}{\partial t^2} \quad (11)$$

$\bar{\lambda}, \bar{\mu}, \bar{\kappa}, \bar{\alpha}, \bar{\beta}$ and $\bar{\gamma}$ materials constants for solid-liquid aggregate, $\bar{\rho}$ is density, \bar{b} is the dissipation function, $\bar{\rho}_{11}, \bar{\rho}_{21}, \bar{\rho}_{22}$ and $\bar{\gamma}$ are the rotation inertia, $\bar{\Phi}$ is microrotation vector, $\bar{\mathbf{u}}$ is the displacement vector in the solid part with components $\bar{u}_1, \bar{u}_2, \bar{u}_3$; $\bar{\mathbf{U}}$ is the displacement vector in the liquid part with components $\bar{U}_1, \bar{U}_2, \bar{U}_3$; $\bar{\mathbf{e}} = \text{div } \bar{\mathbf{u}}, \bar{\mathbf{e}} = \text{div } \bar{\mathbf{U}}, \bar{Q}$ is the measure of coupling between volume change of solid and that of liquid, \bar{R} is the measure of pressure that must exerted on the fluid to force a given volume of it into the aggregate while total volume remains constant.

Let us consider the time harmonic variations ($e^{-i\omega t}$) and assuming the Helmholtz's resolution of displacement vector as

$$\bar{\mathbf{u}} = \nabla \bar{q} + \nabla \times \bar{\mathbf{H}} \quad \nabla \cdot \bar{\mathbf{H}} = 0 \quad (12)$$

$$\bar{\mathbf{U}} = \nabla \bar{g} + \nabla \times \bar{\mathbf{G}} \quad \nabla \cdot \bar{\mathbf{G}} = 0 \quad (13)$$

and eliminating $\bar{\psi}, \nabla^2 \bar{\psi}, \bar{\Phi}_2, \nabla^2 \bar{\Phi}_2$ from the consequential terms and obtained the subsequent equations:

$$(\bar{A}\nabla^4 + \bar{B}\omega\nabla^2 + \bar{C}\omega^4)\bar{q} = 0 \quad (14)$$

$$\bar{A}\nabla^2 + \omega^2(\bar{R}\bar{\rho}_{11} - \bar{\rho}_{12}\bar{Q}) + i\omega(\bar{R} + \bar{Q})\bar{q} - \omega^2\bar{F}\bar{\psi} = 0 \quad (15)$$

$$(\nabla^4 + \bar{D}\omega^2\nabla^2 + \bar{\omega}^4\bar{E})\bar{H}^* = 0 \quad (16)$$

$$\nabla^2(\nabla^2 + \omega^2\bar{E}_2 + \bar{p}\bar{r}_2)\bar{H}^* - \bar{p}(-r_0 + \bar{r}_1\omega^2)\bar{\Phi}_2 = 0 \quad (17)$$

Consider the solution of Eqn. (14) as

$$\bar{q} = \bar{q}_1^* + \bar{q}_2^* \quad (18)$$

where \bar{q}_1^* and \bar{q}_2^* satisfy

$$(\nabla^2 + \bar{\delta}_1^2)\bar{q}_1^* = 0 \quad (\nabla^2 + \bar{\delta}_2^2)\bar{q}_2^* = 0 \quad (19)$$

where

$$\bar{\delta}_{1,2}^2 = \bar{\lambda}_{1,2}\omega^2 \quad \bar{\lambda}_{1,2}^2 = \frac{[\bar{B} \pm \sqrt{(\bar{B}^2 - 4\bar{A}\bar{C})}]}{2\bar{A}}$$

Consequently in limitless medium, solutions of Eqn. (14) correspond to two coupled longitudinal waves. The wave corresponding to \bar{q}_1^* being the faster one is called fast longitudinal displacement (FLD) wave propagating with the phase velocity $\bar{\lambda}_1^2$ and corresponding to \bar{q}_2^* being the slower one, is called slow longitudinal displacement (SLD) wave propagating with the phase velocity $\bar{\lambda}_2^2$.

Using the Eqns. (18) and (17), from the Eqn. (15) obtained the result

$$\bar{\psi} = \bar{\mu}_1\bar{q}_1^* + \bar{\mu}_2\bar{q}_2^* \quad (20)$$

where

$$\bar{\mu}_i = \frac{1}{\bar{F}}(-\bar{A}\bar{\lambda}_i^2 + (\bar{R}\bar{\rho}_{11} - \bar{\rho}_{12}\bar{Q}) + \frac{i\bar{b}}{\omega}(\bar{R} + \bar{Q})\bar{q}_i^*) \quad i=1, 2$$

Consider the solution of equation

$$\bar{\mathbf{H}} = \bar{H}_1^* + \bar{H}_2^* \quad (21)$$

Where \bar{H}_1^* and \bar{H}_2^* satisfy

$$(\nabla^2 + \bar{\delta}_3^2)\bar{H}_1^* = 0 \quad (\nabla^2 + \bar{\delta}_4^2)\bar{H}_2^* = 0 \quad (22)$$

where

$$\bar{\delta}_{3,4}^2 = \bar{\lambda}_{3,4}^2\omega^2 \quad \bar{\lambda}_{3,4}^2 = \frac{[\bar{D} \pm \sqrt{(\bar{D}^2 - 4\bar{E}^2)}]}{2}$$

Using Eqns. (21) and (22) in Eqn. (16), we get

$$\bar{\Phi}_2 = \bar{\mu}_3\bar{H}_1^* + \bar{\mu}_4\bar{H}_2^* \quad (23)$$

where

$$\bar{\mu}_{3,4} = \frac{\bar{\delta}_{3,4}^2(\bar{\delta}_{3,4}^2 - \omega^2\bar{E}^2 - \bar{p}\bar{r}_2)}{\bar{p}(-r_0 + \bar{r}_1\omega^2)}$$

Eventually, in limitless medium, the solutions of Eqn. (22) correspond to two coupled transverse and micro-rotational waves propagating with velocities $\bar{\lambda}_3^2$ and $\bar{\lambda}_4^2$. The following relations in micropolar fluid saturated porous solid are given by Eringen and Konczak

$$\bar{t}_{kl} = (\bar{\lambda}\bar{u}_{r,r} + \bar{Q}\bar{U}_{r,r})\bar{\delta}_{kl} + \bar{\mu}(\bar{u}_{k,l} + \bar{u}_{l,k}) + \bar{\kappa}(\bar{u}_{l,k} - \epsilon_{klr}\bar{\Phi}_r) \quad (24)$$

$$\bar{m}_{kl} = \bar{\alpha}\bar{\Phi}_{r,r}\bar{\delta}_{kl} + \bar{\beta}\bar{\Phi}_{k,l} + \bar{\gamma}\bar{\Phi}_{l,k} \quad (25)$$

$$\sigma = \bar{Q}\bar{\mathbf{e}} + \bar{R}\bar{\mathbf{e}} \quad (26)$$

where $\bar{t}_{kl}, \bar{m}_{kl}$ and σ are represents the force stress, couple stress and the normal stress in liquid respectively.

III. FORMULATION OF THE PROBLEM WHEN INTERFACE $z = 0$ CONTACT PERFECTLY

Now, in this problem by taking z-axis as the interface $z = 0$ perfect in contact separates the micropolar elastic solid, medium M₁ [$z > 0$] and micropolar fluid saturated porous elastic solid, medium M₂ [$z < 0$] as shown in Fig. 1.

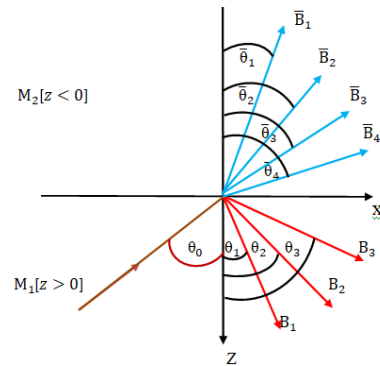


Fig. 1. Geometry of the problem.

The velocity potentials for medium M₁ are taken from Singh and Kumar [22].

The velocity potentials for medium M₂ are derived by Singh and Barak [23].

IV. BOUNDARY CONDITIONS FOR WELDED CONTACT INTERFACE

At the interface $z = 0$, between micro polar elastic solid and micropolar fluid saturated porous solid is considered to be in perfect. The pertinent boundary conditions are continuity of force stresses, couple stress, vanishing of the normal stress in liquid, microrotation and displacements in that order and boundary condition are

At the boundary $z = 0$,

$$\begin{aligned} t_{zz} &= \bar{t}_{zz} & t_{zx} &= \bar{t}_{zx} \\ m_{zy} &= \bar{m}_{zy} & \sigma &= 0 \\ \Phi_2 &= \bar{\Phi}_2 & u &= \bar{u} \\ w &= \bar{w} \end{aligned} \quad (27)$$

Using the expressions of potentials and boundary conditions (27) and using the Snell's law:

$$\frac{\sin \theta_0}{V_0} = \frac{\sin \theta_1}{V_1} = \frac{\sin \theta_2}{\lambda_1^{-1}} = \frac{\sin \theta_3}{\lambda_2^{-1}}$$

$$= \frac{\sin \bar{\theta}_1}{\bar{V}_1} = \frac{\sin \bar{\theta}_2}{\bar{\lambda}_1^{-1}} = \frac{\sin \bar{\theta}_3}{\bar{\lambda}_2^{-1}} \quad (28)$$

where

$$V_0 = \begin{cases} V_1 & \text{for incident longitudinal wave} \\ \lambda_1^{-1} & \text{for incident coupled wave} \end{cases}$$

Eventually, obtained a non-homogeneous system of seven equations in matrix form

$$AZ = B \quad (29)$$

$$Z = [Z_1 Z_2 Z_3 Z_4 Z_5 Z_6 Z_7]^t \quad (30)$$

$$Z_1 = \frac{B_1}{B_0} \quad Z_2 = \frac{B_2}{B_0} \quad Z_3 = \frac{B_3}{B_0} \quad Z_4 = \frac{\bar{B}_1}{B_0}$$

$$Z_5 = \frac{\bar{B}_2}{B_0} \quad Z_6 = \frac{\bar{B}_3}{B_0} \quad Z_7 = \frac{\bar{B}_4}{B_0} \quad (31)$$

where Z_1 to Z_7 are the amplitude ratios of reflected longitudinal displacement, reflected transverse and microrotational waves and refracted FLD, refracted SLD and refracted transverse and microrotational waves.

The coefficients of matrix are:

$$a_{11} = -\{(\lambda + 2\mu + \kappa)\cos^2\theta_1 + \lambda\sin^2\theta_1\}$$

$$a_{12} = -(2\mu + \kappa)\sin\theta_2\cos\theta_2\frac{\bar{\delta}_1^2}{k_*^2}$$

$$a_{13} = -(2\mu + \kappa)\sin\theta_3\cos\theta_3\frac{\bar{\delta}_2^2}{k_*^2}$$

$$a_{14} = \{(2\bar{\mu} + \bar{\kappa})\cos^2\bar{\theta}_1 + \bar{\lambda} + \bar{Q}\bar{\mu}_1\}\frac{\bar{\delta}_1^2}{k_*^2}$$

$$a_{15} = \{(2\bar{\mu} + \bar{\kappa})\cos^2\bar{\theta}_1 + \bar{\lambda} + \bar{Q}\bar{\mu}_1\}\frac{\bar{\delta}_2^2}{k_*^2}$$

$$a_{16} = (2\bar{\mu} + \bar{\kappa})\sin\bar{\theta}_3\cos\bar{\theta}_3\frac{\bar{\delta}_3^2}{k_*^2}$$

$$a_{17} = (2\bar{\mu} + \bar{\kappa})\sin\bar{\theta}_4\cos\bar{\theta}_4\frac{\bar{\delta}_4^2}{k_*^2}$$

$$a_{21} = -(2\mu + \kappa)\sin\theta_1\cos\theta_1$$

$$a_{22} = -\left\{\mu(\cos^2\theta_2 - \sin^2\theta_2) + \kappa\cos^2\theta_2 - \frac{\kappa E}{\bar{\delta}_1^2}\right\}\frac{\bar{\delta}_1^2}{k_*^2}$$

$$a_{23} = -\left\{\mu(\cos^2\theta_3 - \sin^2\theta_3) + \kappa\cos^2\theta_3 - \frac{\kappa F}{\bar{\delta}_2^2}\right\}\frac{\bar{\delta}_2^2}{k_*^2}$$

$$a_{24} = -\{(2\bar{\mu} + \bar{\kappa})\sin\bar{\theta}_1\cos\bar{\theta}_1\}\frac{\bar{\delta}_1^2}{k_*^2}$$

$$a_{25} = -\{(2\bar{\mu} + \bar{\kappa})\sin\bar{\theta}_2\cos\bar{\theta}_2\}\frac{\bar{\delta}_1^2}{k_*^2}$$

$$a_{26} = -\left\{\bar{\mu}(\cos^2\bar{\theta}_3 - \sin^2\bar{\theta}_3) + \bar{\kappa}\cos^2\bar{\theta}_3 - \frac{\bar{\kappa}\bar{\mu}_3}{\bar{\delta}_3^2}\right\}\frac{\bar{\delta}_3^2}{k_*^2}$$

$$a_{27} = -\left\{\bar{\mu}(\cos^2\bar{\theta}_4 - \sin^2\bar{\theta}_4) + \bar{\kappa}\cos^2\bar{\theta}_4 - \frac{\bar{\kappa}\bar{\mu}_4}{\bar{\delta}_4^2}\right\}\frac{\bar{\delta}_4^2}{k_*^2}$$

$$a_{31} = a_{34} = a_{35} = 0, a_{32} = \lambda E \bar{\delta}_1 \cos\theta_2$$

$$a_{33} = \lambda F \bar{\delta}_2 \cos\theta_3, a_{36} = \bar{\lambda} \bar{\mu}_3 \bar{\delta}_3 \cos\bar{\theta}_3$$

$$a_{37} = \bar{\lambda} \bar{\mu}_4 \bar{\delta}_4 \cos\bar{\theta}_4$$

$$a_{41} = a_{42} = a_{43} = a_{46} = a_{47} = 0$$

$$a_{44} = (\bar{Q} + \bar{\mu}_1 \bar{R}), a_{45} = (\bar{Q} + \bar{\mu}_2 \bar{R})$$

$$a_{51} = a_{54} = a_{55} = 0, a_{52} = E a_{53} = F$$

$$a_{56} = -\bar{\mu}_3 a_{57} = -\bar{\mu}_4, a_{61} = -i \sin\theta_1$$

$$a_{62} = i \cos\theta_2 \frac{\bar{\delta}_1}{k_*}, a_{63} = i \cos\theta_3 \frac{\bar{\delta}_2}{k_*}$$

$$a_{64} = i \sin\bar{\theta}_1 \frac{\bar{\delta}_1}{k_*}, a_{65} = i \sin\bar{\theta}_2 \frac{\bar{\delta}_2}{k_*}$$

$$a_{66} = -\cos\bar{\theta}_3 \frac{\bar{\delta}_3}{k_*}, a_{67} = -\cos\bar{\theta}_4 \frac{\bar{\delta}_4}{k_*}$$

$$a_{71} = \cos\theta_1 a_{72} = i \sin\theta_2 \frac{\bar{\delta}_1}{k_*} a_{73} = i \sin\theta_3 \frac{\bar{\delta}_2}{k_*}$$

$$a_{74} = \cos\bar{\theta}_1 \frac{\bar{\delta}_1}{k_*} a_{75} = \cos\bar{\theta}_2 \frac{\bar{\delta}_2}{k_*} a_{76} = \sin\bar{\theta}_3 \frac{\bar{\delta}_3}{k_*}$$

$$a_{77} = \cos\bar{\theta}_4 \frac{\bar{\delta}_4}{k_*} \quad (32)$$

where

(i) For the incident longitudinal wave ($k_* = k_0$)

$$Y_1 = -a_{11} \quad Y_2 = a_{21} \quad Y_3 = a_{31}$$

$$Y_4 = a_{41} \quad Y_5 = -a_{51} \quad Y_6 = -a_{61}$$

$$Y_7 = a_{71} \quad (33)$$

(ii) For the incident coupled wave ($k_* = \bar{\delta}_1$)

$$Y_1 = a_{12} \quad Y_2 = -a_{22} \quad Y_3 = a_{32}$$

$$Y_4 = a_{42} \quad Y_5 = -a_{52} \quad Y_6 = a_{62}$$

$$Y_7 = -a_{72} \quad (34)$$

V. NUMERICAL RESULTS AND DISCUSSION

System of seven non-homogeneous equations obtained above is solved by Cramer rule to obtain the various amplitude ratios for emergence longitudinal wave as well as coupled wave. In order to understand the behavior of different amplitude ratios and revealed in graphically and by taking the values of applicable elastic parameters.

For M_1 , Gauthier [24], derived the parametric values for medium M_1 .

$$\lambda = 7.59 \times 10^{11} \text{ dyne/cm}^2 \quad \mu = 1.89 \times 10^{11} \text{ dyne/cm}^2$$

$$\kappa = 0.0149 \times 10^{11} \text{ dyne/cm}^2 \quad \rho = 2.19 \text{ gm/cm}^3$$

$$\gamma = 0.0268 \times 10^{11} \text{ dyne} \quad j = 0.0196 \text{ cm}^2$$

$$\bar{\omega}^2 / \bar{\omega}_0^2 = 20 \quad (35)$$

For medium M_2 , a particular modal micropolar fluid saturated porous solid, the physical constants are given by Gauthier [24]

$$\bar{\lambda} = 4.339 \times 10^5 \text{ N/cm}^2 \quad \bar{\mu} = 2.765 \times 10^5 \text{ N/cm}^2$$

$$\bar{\kappa} = 1.49 \times 10^4 \text{ N/cm}^2 \quad \bar{\gamma} = 2.68 \times 10^5 \text{ dyne}$$

$$\bar{j} = 2 \times 10^{-16} \text{ cm}^2 \quad \bar{\rho} = 2.19 \text{ gm/cm}^3$$

$$\rho_{11} = 2.1372 \text{ gm/cm}^3 \quad \rho_{11} = 1.926137 \text{ gm/cm}^3$$

$$\rho_{12} = -0.002137 \text{ gm/cm}^3 \quad \rho_{22} = 0.215337 \text{ gm/cm}^3$$

$$\bar{Q} = 7.635 \times 10^4 \text{ N/cm}^3 \quad \bar{R} = 3.26 \times 10^4 \text{ N/cm}^3$$

$$\bar{\omega}^2 = 10 \quad f = \frac{b}{\rho_1 \omega} = 0.712547 \quad (36)$$

Determines the amplitude ratios of different waves for this especially model and using the MATLAB software (R2015a 32-bit) for executing the program and revealed figurewise.

In Figs. (2-11), describes the variations of amplitude ratios with the different emergence wave, first wave is longitudinal wave and second one is coupled wave respectively, solid lines show the variations of $|Z_i|$, M_1 is micropolar elastic solid and M_2 is micropolar fluid saturated porous solid. This case is represented by 'General' and uses its abbreviation "GEN" in the figures. The tendency of $|Z_i|$ is based on incident wave with different angles.

In Fig. 2, the dissimilarity in the values of $|Z_1|$ is non-zero at initial angle *i.e.* $\theta_0 = 0^\circ$ and final angle *i.e.* $\theta_0 = 90^\circ$ whereas the values of $|Z_2|$ and $|Z_3|$ are zero at initial and final angle. Now, the values of $|Z_1|$ are smoothly decreases from its maxima $\theta_0 = 0^\circ$ and approaches to minimum value at the angle $\theta_0 = 68^\circ$ but after that values are rapidly increases from the same point and approaches to maxima at the angle $\theta_0 = 90^\circ$. On the other hand, the values of $|Z_2|$ are smoothly increases from the initial angle $\theta_0 = 0^\circ$ and obtain its maximum value approximately at $\theta_0 = 54^\circ$ and later values are very slowly decreases corresponding to angle of emergence and approaches to minima at $\theta_0 = 90^\circ$. The values of

$|Z_3|$ are very low in contrast to the $|Z_1|$ and $|Z_2|$ and values are increases and decreases according to angles. The values of $|Z_1|$, $|Z_2|$ and $|Z_3|$ are totally different to each others except some angle. In this figure, the value of amplitude ratio $|Z_1|$ is higher than $|Z_2|$ and $|Z_3|$.

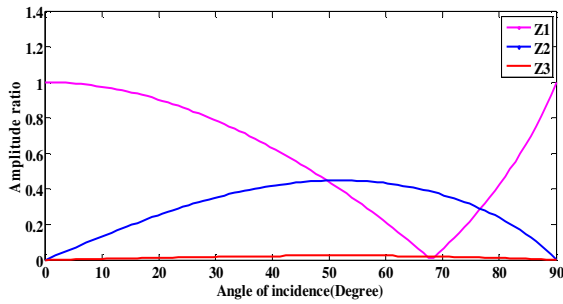


Fig. 2. Variations of amplitude ratios against Degree for longitudinal waves for amplitude ratio 1, 2, 3.

The Fig. 3, describes the variation of the values of $|Z_4|$. In the beginning the value is non-zero and maximum at initial angle *i.e.* $\theta_0 = 0^\circ$ and zero at final angle *i.e.* $\theta_0 = 90^\circ$. Now, the values of $|Z_4|$ are smoothly decreases from its local maxima $\theta_0 = 0^\circ$ and approaches to minimum value at the angle $\theta_0 = 90^\circ$.

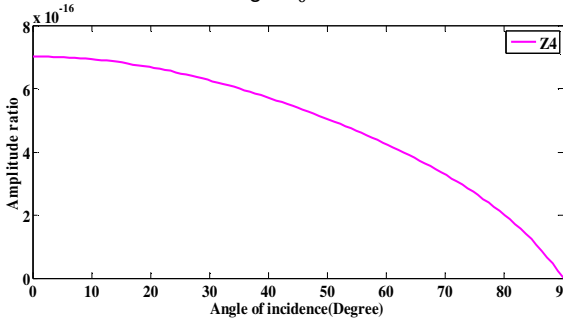


Fig. 3. Variations of amplitude ratios against Degree for longitudinal waves for amplitude ratio 4.

In Fig. 4, shows the dissimilarity of the values of $|Z_5|$. In the beginning the value is non-zero and maximum at initial angle *i.e.* $\theta_0 = 0^\circ$ and zero at final angle *i.e.* $\theta_0 = 90^\circ$. Now, the values of $|Z_5|$ are smoothly decreases from its maximum value at the angle $\theta_0 = 0^\circ$ and approaches to minimum value at the angle $\theta_0 = 90^\circ$.

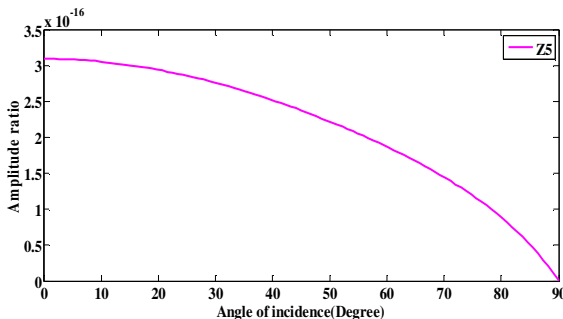


Fig. 4. Variations of amplitude ratios against Degree for longitudinal waves for amplitude ratio 5.

The Fig. 5, describes the variation of the values of $|Z_6|$. The values of $|Z_6|$ are zero and minimum at the initial and final angle *i.e.* $\theta_0 = 0^\circ$ and $\theta_0 = 90^\circ$. The values are

smoothly increases from the initial angle $\theta_0 = 0^\circ$ of $|Z_6|$ and obtain its maximum value approximately at $\theta_0 = 53^\circ$ but after that the values are sharply decreases as well as angle of emergence are increases and approaches to minima at $\theta_0 = 90^\circ$.

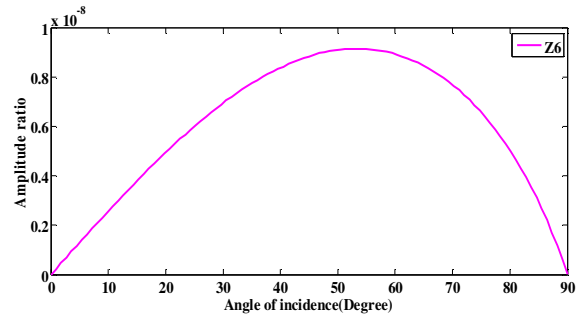


Fig. 5. Variations of amplitude ratios against Degree for longitudinal waves for amplitude ratio 6.

In this Fig. 6, describes the dissimilarity of the values of $|Z_7|$. The values of $|Z_7|$ are zero at the initial and final angle *i.e.* $\theta_0 = 0^\circ$ and $\theta_0 = 90^\circ$. From the angle of incidence $\theta_0 = 0^\circ$ the values are smoothly increases and obtain its local maxima approximately at $\theta_0 = 54^\circ$ whereas the values are sharply decreases as well as angle of emergence are increases and approach to its minima at $\theta_0 = 90^\circ$.

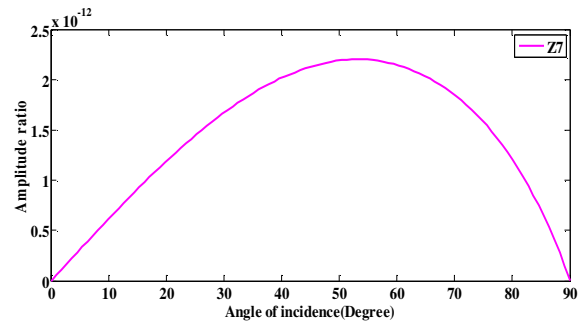


Fig. 6. Variations of amplitude ratios against Degree for longitudinal waves for amplitude ratio 7.

In the Fig. 7, dispersion in amplitude ratios $|Z_i|$ ($i = 1, 2, 3$) is depicted in GEN case when the incidence angle varies from $\theta_0 = 0^\circ$ to 90° . The value of $|Z_1|$ is zero when $\theta_0 = 0^\circ$ and $\theta_0 = 90^\circ$ while the value of $|Z_3|$ is zero only at the angle $\theta_0 = 90^\circ$ and value of $|Z_2|$ is non-zero at $\theta_0 = 0^\circ$ and $\theta_0 = 90^\circ$. Now, the values of amplitude ratio $|Z_1|$ sharply increasing continuously when emergence angle increases from its initial position to the angle $\theta_0 = 24^\circ$ after that the values are sharply decreasing from the same highest value when emergence angle increases from the angle $\theta_0 = 24^\circ$ to $\theta_0 = 90^\circ$. The values of $|Z_2|$ are smoothly decreases when the angle $\theta_0 = 0^\circ$ and approaches to minimum value at the angle $\theta_0 = 20^\circ$ but after that values are sharply increases from the same point and approaches to maxima at the angle $\theta_0 = 24^\circ$ and again values are sharply decreases from the peak point to angle $\theta_0 = 27^\circ$ and then values are very slowly decreases and increases according to increases the angle of incidence. The values of $|Z_3|$ are very less in comparison to the $|Z_1|$ and $|Z_2|$ and values are increases and decreases according to angle. The values of $|Z_1|$, $|Z_2|$ and $|Z_3|$ are totally different to each

others except some angle. In this figure, the maximum value of amplitude ratio $|Z_1|$ is higher than $|Z_2|$ and $|Z_3|$ and the greatest value of $|Z_2|$ is higher than $|Z_3|$.

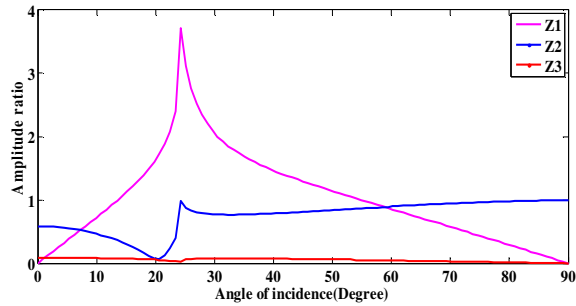


Fig. 7. Variations of amplitude ratios against Degree for coupled waves for amplitude ratios 1, 2, 3.

In the Fig. 8, dispersion in amplitude ratios $|Z_4|$ is depicted in GEN case when the incidence angle varies from $\theta_0 = 0^\circ$ to 90° . The value of $|Z_4|$ is zero when $\theta_0 = 0^\circ$ and $\theta_0 = 90^\circ$. Now, the values of amplitude ratio $|Z_4|$ sharply increasing continuously when emergence angle increases from its initial position to the angle $\theta_0 = 24^\circ$ after that the values are sharply decreasing from the same highest value when emergence angle increases from the angle $\theta_0 = 24^\circ$ to $\theta_0 = 90^\circ$.

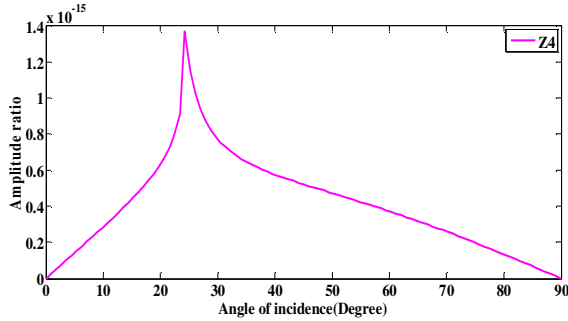


Fig. 8. Variations of amplitude ratios against Degree for coupled waves for amplitude ratio 4.

In the Fig. 9, dispersion in amplitude ratios $|Z_5|$ is depicted in GEN case when the incidence angle varies from $\theta_0 = 0^\circ$ to $\theta_0 = 90^\circ$. Despite the different values of $|Z_4|$ and $|Z_5|$ except only the angles $\theta_0 = 0^\circ$ and 90° , the behaviour of the in Fig. 7, 8 is similar.

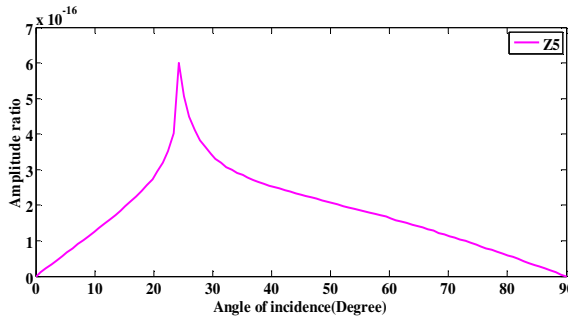


Fig. 9. Variations of amplitude ratios against Degree for coupled waves for amplitude ratio 5.

In this Fig. 10, describes the variation of the values of $|Z_6|$. At the beginning the value is non-zero and maximum at initial angle *i.e.* $\theta_0 = 0^\circ$ and zero at final

angle *i.e.* $\theta_0 = 90^\circ$. Now, the values of amplitude ratio $|Z_6|$ are smoothly decreases from its maximum value at the angle of incidence $\theta_0 = 0^\circ$ to $\theta_0 = 24^\circ$ but after that values are suddenly increases $\theta_0 = 24^\circ$ to $\theta_0 = 26^\circ$ and again decreases when angle of incidence are increases and approaches to minimum value at the angle $\theta_0 = 90^\circ$.

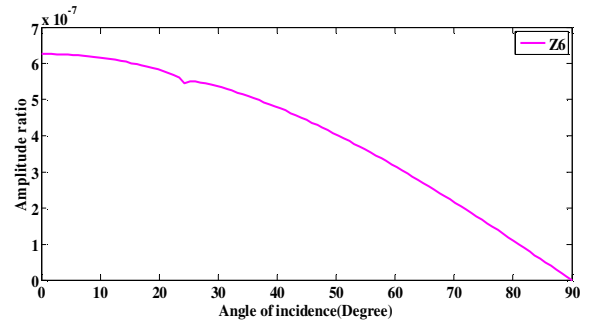


Fig. 10. Variations of amplitude ratios against Degree for coupled waves for amplitude ratio 6.

In the Fig. 11, variation in the values of $|Z_7|$ is depicted in GEN case when the angle varies from $\theta_0 = 0^\circ$ to $\theta_0 = 90^\circ$. The behaviour of the in Fig. 10, 11 is similar with the different values of $|Z_6|$ and $|Z_7|$ except only the angle $\theta_0 = 90^\circ$.

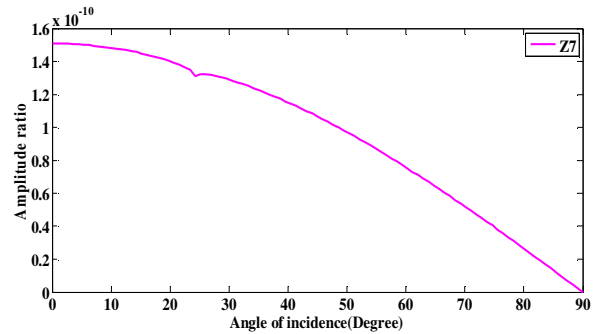


Fig. 11. Variations of amplitude ratios against Degree for coupled waves for amplitude ratio 7.

VI. CONCLUSION

In this mathematical problem, decomposing micropolar elastic solid and micropolar fluid saturated porous solid at interface. We have observed that

- The amplitudes ratios of various waves are with the complex valued.
- The tendency of amplitudes ratios of various waves depending at angle θ_0 and the incident wave and properties of materials half spaces.
- The behaviors of some figures of amplitude ratios are remain same whereas the values are totally different.

CONFLICT OF INTEREST

Author has no any conflict of interest.

REFERENCES

- [1]. Eringen, A. C., & Suhubi, E. S., (1964). Non linear theory of simple micro-elastic solids I. *International Journal of Engineering Science*, Vol. 2, 189-203.
- [2]. Eringen, A.C., Micropolar elastic solids with stretch. *Ari. KitabeviMatabaasi*, Vol. 24 :1-9.
- [3]. Parfitt, V. R., & Eringen, A. C., (1969). Reflection of plane waves from the flat boundary of a micropolar

- elastic half space. *J. Acoust. Soc. Am.*, Vol. **45**, 1258-1272.
- [4]. Nowacki, W., (1974). The Linear Theory of Micropolar Elasticity. *International Centre for Mechanical Sciences, Springer, New York*.
- [5]. Tomar, S.K., & Gogna, M.L., (1992). Reflection and refraction of longitudinal microrotational wave at an interface between two different micropolar elastic solids in welded contact. *International Journal of Engineering Science*, Vol. **30**, 1637-1646.
- [6]. Kumari, N., (2013). Wave propagation at micropolar elastic/fluid saturated porous solid interface. *International Journal of Mathematical Archive*, Vol. **4**(8), 56-66.
- [7]. Barak, M., Kumari, N., & Kaliraman, V., (2015). Reflection and Refraction of Wave in two welded contact infinite unbounded half Spaces. *International Journal of Research in Engineering and Applied Sciences*, Vol. **5**(3): 84-100.
- [8]. Merkel, A., & Luding, S., (2017). Enhance micropolar model for wave propagation in ordered granular materials. *International Journal of Solids and Structures*, Vol. **106-107**, 91-105.
- [9]. Kumari, N., Kumar, P., & Kaliraman, V., (2018). Analysis of wave propagation between solid-solid interfaces. *International Journal of Statistika and Matematika*, Vol. **25**(1): 24-33.
- [10]. Kumar, R., Madan, D. K. & Sikka, J.S. (2014). Shear wave propagation in multilayered medium including an irregular fluid saturated porous stratum with rigid boundary. *Advances in Mathematical Physics*, Article ID 163505, 9 pages.
- [11]. Kumar, R., Madan, D. K. & Sikka, J.S. (2015). Wave propagation in an irregular fluid saturated porous anisotropic layer sandwiched between a homogeneous layer and half space. *WSEAS Transaction on Applied and Theoretical Mechanics*, **10**: 62-70.
- [12]. Kumar, R., Madan, D. K. & Sikka, J. S. (2015). Effect of irregularity and inhomogeneity on the propagation of Love waves in fluid saturated porous isotropic layer. *Journal of Applied Science and Technology*, **20**(1-2): 16 – 21.
- [13]. Kumar, R., Madan, D.K. & Sikka, J. S. (2015). Effect of irregularity and anisotropy on the propagation of shear waves: A review. *Proceedings of Second IRF International Conference, Pondicherry, India*, **4**: 16-19.
- [14]. Kumar, R., Madan, D. K. & Sikka, J. S. (2016). Effect of rigidity and inhomogeneity on the propagation of Love waves in an irregular fluid saturated porous isotropic layer. *International Journal of Mathematics and Computations*, **27**(2): 55-70.
- [15]. Madan, D. K., Kumar, R., & Sikka, J.S. (2014). Love wave propagation in an irregular fluid saturated porous anisotropic layer with rigid boundary. *J. Appl. Sci. Res.*, **10**(4), 281–287.
- [15]. Madan, D. K., Kumar, R., & Sikka, J. S. (2017). The propagation of surface waves in a double layered medium over an anisotropic liquid saturated porous half space. *Bulletin of Pure & Applied Sciences-Geology*, **36F**(2): 87-102.
- [16]. Madan, D. K., Kumar, R. & Sikka, J. S. (2017). The propagation of love waves in an irregular fluid saturated porous anisotropic layer. *Global Journal of Pure and Applied Mathematics*, **13**(1): 63-80.
- [17]. Kaliraman, V. & Poonia, R.K. (2018). Elastic wave propagation at imperfect boundary of micropolar elastic solid and fluid saturated porous solid half-space. *Journal of Solid Mechanics*, **10**(3): 655-671.
- [18]. Biot, M. A. (1955): Theory of elasticity and consolidation for a porous anisotropic solid. *J. Appl. Phys.* **26**: 182-185.
- [19]. Biot M. A. (1956). Theory of propagation of elastic waves in a fluid- saturated porous solid. *J. Acoustic. Soc. Am.* **28**: 168-178.
- [20]. Eringen, A.C., (1968). Theory of micropolar elasticity. *Fracture (New York: Academic Press)* Vol. **2**.
- [21]. Singh, B., & Kumar, R., (2007). Wave reflection at viscoelastic-micropolar elastic interface. *Applied Mathematics and Computation*, **185**, 421-431.
- [22]. Singh, B., (2000). Reflection and transmission of plane harmonic waves at an interface between liquid and micropolar viscoelastic solid with stretch. *Sadhana*, Vol. **25**, 589-600.
- [23]. Gauthier, R. D., (1982). Experimental investigations on micropolar media. *Mechanics of micropolar media (eds) O Brulin, R K T Hsieh (World Scientific, Singapore)*, p. 395.